

2D.5 ON THE SLOWDOWN OF LANDFALL TYPHOON BY TOPOGRAPHY PHASE LOCKED CONVECTIONS

Li-Huan Hsu¹, Hung-Chi Kuo^{1*}, Robert G. Fovell², Yu-Han Chen¹ and Tse-Chun Chen¹

¹Department of Atmospheric Sciences, National Taiwan University, Taipei, Taiwan

²Department of Atmospheric and Ocean Sciences, University of California, Los Angeles, Los Angeles

1 Introduction

Taiwan is a mountainous island 150 km in width and 400 km in length, with the peak altitude of the Central Mountain Range (CMR) exceeding 3000 m. The annual precipitation of Taiwan is approximately 2500 mm, with most of the heavy rainfall resulting from typhoons. The typhoon rainfall pattern is phase-locked with the CMR, with its southwest slope receiving especially large amounts for typhoons located northern than 23 °N (Chang et al. 1993). Typhoon Morakot (2009), while not a notable storm with respect to maximum wind speeds, its slow translation speed and ample moisture supplied by the southwest monsoon are two key reasons why that typhoon produced the largest recorded rainfall in Taiwan in the past 30 years (Chien and Kuo 2011). This study examines the effect of the topography phase-locked convection on the typhoon motion crossing the island of Taiwan.

2 Observation

Westward typhoons with continuous track (61 cases) that made landfall in Taiwan are analyzed from 1960 to 2010. Hourly typhoon center positions and the intensity of typhoons, which is defined as the maximum wind speed of typhoon within one degree of Taiwan, are collected from typhoon database (Wang 1980; Shieh et al. 1998) of Central Weather Bureau, Taiwan (CWB). With landfall/departure positions and

times, translation speeds for each typhoon are obtained. We define the speed criteria as slow and fast cases with the mean translation speed of 61 continuous cases (6.2 m s^{-1}) plus/minus one standard deviation 2.9 m s^{-1} .

For 61 continuous cases, a significant geographic asymmetry exists with respect to typhoon overland translation, with 77 % (10 of 13) of the slow moving storms making landfall on the northern (greater than 23.5 °N; hereafter NLT) segment of Taiwan's east coast and 60 % (6 of 10) of the fast cases reaching the southern (less than 23.5 °N; hereafter SLT) segment instead.

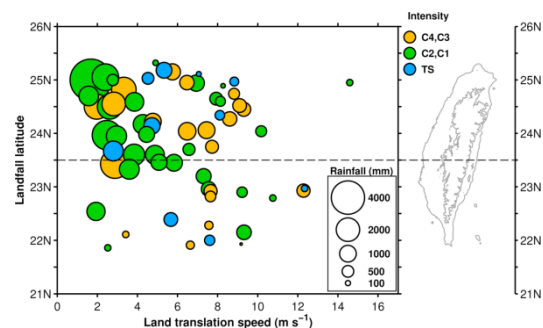


Fig. 1 The rainfall amount (area of circle) overland over 21 CWB surface stations as a function of the translation speed, latitude and maximum storm intensity.

Figure 1 presents total rainfall during the overland period for the 21 CWB surface stations as a function of the translation speed, latitude and maximum storm intensity. The figure emphasizes that more of the slower typhoons are from the NLT and are associated with larger precipitation totals.

* Corresponding author address: Hung-Chi Kuo, Department of Atmospheric Sciences, National Taiwan University, Taipei, Taiwan; e-mail: kuo@as.ntu.edu.tw.

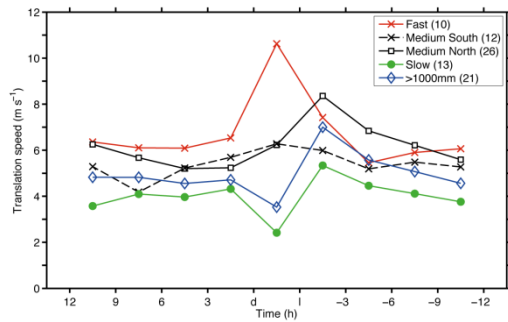


Fig. 2 Three-hourly mean translation speed variations. Red cross, black cross, black squares, green dots and blue diamonds are fast, medium south, medium north, slow and cases with rainfall amount over 1000 mm overland respectively.

Figure 2 shows 3-hourly mean translation speed variations from 12 h before landfall to 12 h after departure. Divide cases as fast, slow, medium and larger rainfall groups. The medium speed class is further subdivided into northern and southern subgroups, again based on their landfall latitude relative to 23.5°N. Note all subgroups accelerate as they approach Taiwan's east coast. Among the medium speed storms, the pre-landfall speed increase is larger in the northern subgroup, and greatest acceleration is seen in the cases that subsequently present the fastest overland motion. After landfall, the slow movers and the medium north subgroup typhoons decelerate markedly. For comparison, we also show the temporal speed variation speeds for typhoon cases that produced total rainfall amounts exceeding 1000 mm while over land.

For all cases combined, the typhoon-produced rainfall tends to be largest in the west side of the CMR, at the Alishan station located near latitude 23.5°N (Fig. 3). The peak is most pronounced in the slow and the medium north group (Figs. 4a, b); none of the fast movers result in more than 50 mm of rain during the post-landfall period (Fig. 4c). The average rainfall at the Alishan station is 325 (162) mm for the slow

(medium north) group typhoons and the sum of 21 surface stations is 2128 (809) mm respectively.

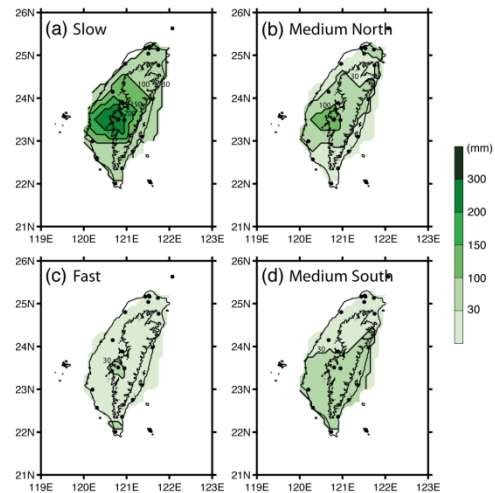


Fig. 3 The mean rainfall amount (mm) (shading) of (a) slow, (b) medium north, (c) fast and (d) medium south typhoons.

3 Model settings and diabatic heating potential vorticity tendency diagnosis

A “semi-idealized” variant of the “real data” WRF model (version 3.1.1) is used. Model physics options selected include the YSU planetary boundary layer scheme, Lin et al. microphysics scheme. The simulations employ a single square domain, 1500 km on a side, and the model top is placed at 10 hPa. The horizontal resolution is 5 km and there are 35 model levels in the vertical. The base state consists of Jordan's (1958) Caribbean hurricane season composite temperature and humidity sounding with a uniform sea surface temperature (SST) of 29°C. The background wind field consists of easterly flow that is uniform in both the horizontal and vertical directions. The typhoons are initialized by the WRF tropical cyclone bogus scheme. This scheme gives the initial vortex a modified Rankine wind profile. The model domain has no topography other than the island of Taiwan, which was constructed using the 30 sec resolution USGS database.

Potential vorticity (PV) tendency diagnosis (Wu and Wong 2000, hereafter WW) is adapted in our analysis in evaluating the diabatic heating effect on the storm motion during the landfall period.

$$\frac{\partial P}{\partial t} = -\mathbf{V} \cdot \nabla_h P - w \frac{\partial P}{\partial z} + \rho^{-1} \nabla_3 \cdot (Q\mathbf{q}), \quad (1)$$

where P is PV, \mathbf{V} is three dimensional wind, ρ is density, Q is diabatic heating, \mathbf{q} is the absolute vorticity and ∇_3 is the three dimensional gradient operator. To test our hypothesis of phase-locked convection slow down the northern typhoons, we will focus particularly on the diabatic heating of the PV tendency (DH).

WW suggest that the azimuthal wavenumber one (WN1) component of PV tendency in a fixed frame is balanced by the advection of the symmetric PV component associated with TC motion. Namely,

$$\left(\frac{\partial P}{\partial t}\right)_1 = -C_x \frac{\partial P_s}{\partial x} - C_y \frac{\partial P_s}{\partial y}, \quad (2)$$

where P_s is symmetric component of the vortex PV, the suffix 1 denotes the WN1 component, and C_x , C_y are scalar speeds in the x and y directions, respectively. In (2), we compute the left hand side of the PV tendency representing the diabatic heating and determine the C_x and C_y via the least square method. The C_x and C_y form a vector representing the magnitude and direction that the DH contributes to the storm motion.

4 Numerical results

Figure 4 compares 3-hourly tracks from a simulation using real Taiwan topography (run T3N) with an oceanic control run (run OC) without the topography. Both commenced with identical bogussed typhoons having a 50 m s^{-1} maximum wind at 50 km radius from the center. The typhoons were initially placed at 20.5°N , 124.5°E , which is 400 km east of Taiwan for the T3N run, embedded in a 3 m s^{-1} uniform mean flow. The shading is the total rainfall

difference between the T3N and OC experiments through 72 hours of model integration. Significant differences emerge as the T3N storm approaches Taiwan. The OC storm's average motion between hours 24 and 28 is 4.2 m s^{-1} . In contrast, the speed of T3N typhoon in the similar location increased from 3.6 m s^{-1} (between 24-28 h) to 5.0 m s^{-1} for hours 32-35 h before landfall. After landfall at northern Taiwan, the T3N storm slows down considerably (1.8 m s^{-1} in average), and spends 22 h (from 35-57 h) over the island. The slowdown appears to be consistent with the observations.

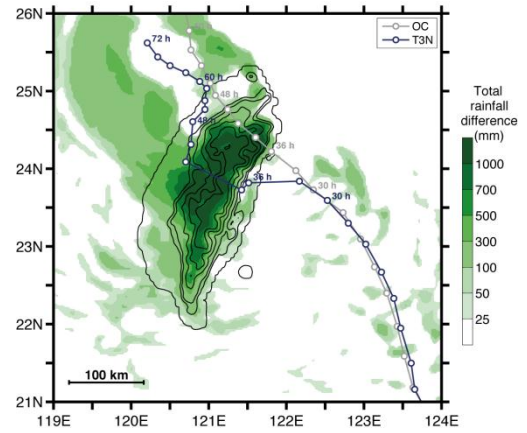


Fig. 4 Three hourly typhoon tracks over 72 h for ocean control (OC) experiment (gray) and Taiwan terrain (T3N) experiment (blue). Shading is the total rainfall difference over 72 h.

Figure 5a and 5c shows the T3N typhoon's moving vector \mathbf{C} , the motion vector contributed by DH component and diabatic heating Q averaging from level 1 to 20 for time periods 24-28 h and 48-57 h respectively. The DH contributed motion vector is small and accompanied with rather symmetric Q and rainfall pattern when the storm is over the ocean (Fig. 6b). Once the typhoon passes west of the CMR, however, DH exerts much more influence on the storm motion, and specifically acts to induce the storm to slow down over land. This is indicated by Fig. 5c

that the diabatic heating Q is in the southwest flank of the storm. This is also indicated in Fig. 5d that rainfall during the 48-57 h period exceeds 3191 mm and in general is concentrated on the typhoon's southwest flank on slope of the CMR terrain. The storm motion is now northward at a substantially reduced speed of 1.6 m s^{-1} .

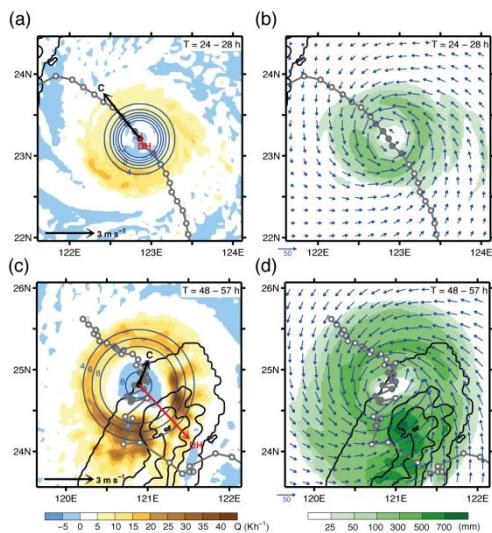


Fig. 5 (a) Vertical averaging of diabatic heating (in colors) and the motion vector of DH (in red), (b) surface wind (blue vectors) and rainfall (in green colors) for 24-28 h of T3N. (c) and (d) are similar with (a), (b) but for 48 to 57 h.

Figure 6 presents the DH contributed along track motion vectors for OC experiment (orange) and for T3N experiment (red). Over the ocean region, both T3N and OC storms are with negligible DH contributions. The OC storm move with a nearly constant speed and the DH vector fluctuated in the late stage of model integration. On the other hand, DH vectors become larger than that of the OC vectors near the landfall. The most significant DH vector occurred in the west of the CMR as discussed in Fig. 5. Figure 6 further supports the argument of topography phase-locked convection slowdown the storm motion in the west of CMR. Figure 7 is the similar experiment as the T3N except the background flow is faster (5 m s^{-1}).

ms^{-1}). Figure 7 suggests that the diabatic heating effect on the slowdown of the storm motion is less significant. This may be due to the reduction of precipitation on the CMR when the storm moves faster. The result may imply that the slower storm with more precipitation may yield an even slower motion, the faster storm may yield less slowdown effect.

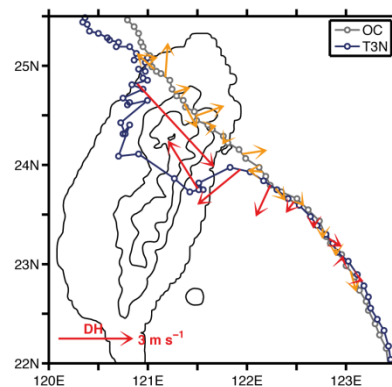


Fig. 6 The DH contributed along track motion vectors for OC experiment (orange) and for T3N experiment (red).

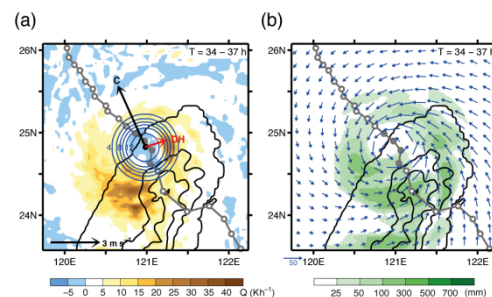


Fig. 7 Same as Fig. 5 but for faster mean flow experiment (5 m s^{-1}) and northern landfall storm.

5 Conclusions

Data for 61 continuous typhoons that reached Taiwan's east coast from 1960 to 2010 are analyzed, with motions compared to the long-term average overland translation speed. We find that 77% of the slow-moving TCs (speed lower than one standard deviation) made landfall on the northeast coast, while 60% of the fast storms (speed faster than one

standard deviation) had southeast coastal landfalls. The geographic asymmetry with respect to typhoon translation speeds widened after landfall, as the slow-movers typically decelerated during the overland period while the faster TCs speed up. The combination of slower translation with longer duration for the northern class of TCs leads to large rainfall on the southwest slope of Central Mountain Range.

WRF Model experiments are used to study the effect of topography phase-locked convection on the storm motion over Taiwan. We compute the the PV tendency due to the diabatic heating, decomposed into the wave number one component and calculate its contributions to the storm motion. Our experiments suggest that the phase-locked convection acts to slow down the northern landfall typhoons west of Central Mountain Range. Our model results also suggest a positive feedback mechanism exists for the slow storms, in which the convective heating pattern forced by topography acts to reduce the TC motion, leading to even more prolonged precipitation and heating, yielding further speed reductions. Further sensitivity experiments are perform

6 References

- Cao, Y., R. G. Fovell, and K. L. Corbosiero, 2011: Tropical cyclone track and structure sensitivity to initialization in idealized simulations: A preliminary study. *Terr. Atmos. Ocean. Sci.*, **22**, 559-578.
- Chang, C. P., T. C. Yeh, and J. M. Chen, 1993: Effects of terrain on the surface structure of typhoons over Taiwan. *Mon. Wea. Rev.*, **121**, 734-752.
- Chien, F. C., and H. C. Kuo, 2011: On the extreme rainfall of typhoon Morakot (2009). *J. Geophys. Res.*, **116**, D05104, doi:10.1029/2010JD015092.
- Shieh, S. L., S. T. Wang, M. D. Cheng, and T. C. Yeh, 1998: Tropical cyclone tracks over Taiwan and its vicinity for the one hundred years 1897 to 1996 (in Chinese). Research Rep. CWB86-1M- 01, Central Weather Bureau, Taipei, Taiwan, 497 pp.
- Wang, S. T., 1980: Prediction of the behavior and intensity of typhoons in Taiwan and its vicinity (in Chinese). Research Rep., 108, Chinese National Science Council, Taipei, Taiwan, 100pp.
- Wu, L., and B. Wang, 2000: A potential vorticity tendency diagnostic approach for tropical cyclone motion. *Mon. Wea. Rev.*, **128**, 1899-1911.